

**SUPPLEMENTARY INFORMATION**

**Accounting for Molecular Flexibility in Photoionization:  
Case of *tert*-Butyl Hydroperoxide**

Jérémy Bourgalais<sup>1,\*</sup>, Zhongming Jiang<sup>2</sup>, Julien Bloino<sup>2</sup>, Olivier Herbinet<sup>1</sup>, Hans-Heinrich Carstensen<sup>3,4</sup>, Gustavo A. Garcia<sup>5</sup>, Philippe Arnoux<sup>1</sup>, Luc-Sy Tran<sup>6</sup>, Guillaume Vanhove<sup>6</sup>, Laurent Nahon<sup>5</sup>, Frédérique Battin-Leclerc<sup>1</sup>, and Majdi Hochlaf<sup>7,\*</sup>

<sup>1</sup>Université de Lorraine, CNRS, LRGP, F-54000 Nancy, France.

<sup>2</sup>SMART Laboratory, Scuola Normale Superiore, Pisa, Italy.

<sup>3</sup>Thermochemical Processes Group (GPT), Department of Chemical and Environmental Engineering, Engineering and Architecture School, University of Zaragoza, Spain

<sup>4</sup>Fundacion Agencia Aragonesa para la Investigacion y el Desarrollo (ARAID), Zaragoza, Spain

<sup>5</sup>Synchrotron SOLEIL, L'Orme des Merisiers, Saint-Aubin-BP 48, 91192 Gif-sur-Yvette Cedex, France

<sup>6</sup>PC2A, Université de Lille, CNRS; Avenue Mendeleiev, 59650 Villeneuve-d'Ascq, France

<sup>7</sup>Université Gustave Eiffel, COSYS/LISIS, 5 Bd Descartes 77454, Champs sur Marne, France

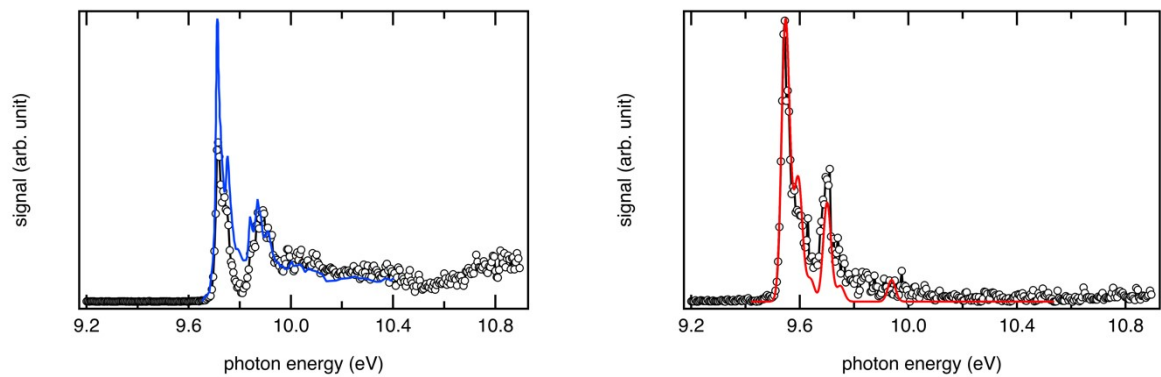


FIGURE S1. (left) SPES of  $m/z$  58 (open circles) recorded during synchrotron photoionization of a tBuOOH/*n*-decane mixture in helium compared to TPES of acetone (blue line) from Rennie et al. [61]; (right) SPES of  $m/z$  72 (black dots) recorded during synchrotron photoionization of a tBuOOH/*n*-decane mixture in helium compared to a simulated PES of methyl ethyl ketone (red line) from Bourgalais et al. [62].

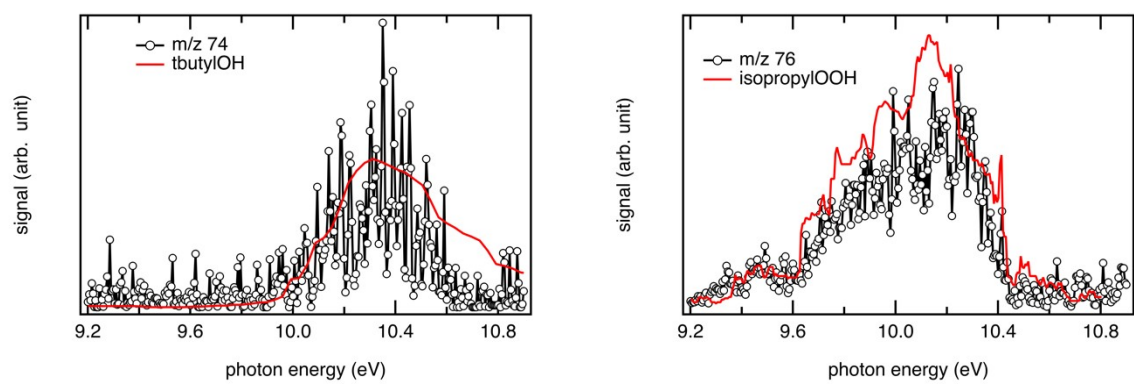


FIGURE S2. (left) SPES of  $m/z$  74 (black dots) recorded during synchrotron photoionization of a tBuOOH/*n*-decane mixture in helium compared to a published spectrum of tBuOH (red line) from Ogata et al. [63]; (right) SPES of  $m/z$  76 (black dots) recorded during synchrotron photoionization of a tBuOOH/*n*-decane mixture in helium compared to the spectrum of isopropyl hydroperoxide (red line) reported by Bierkandt et al. [5].

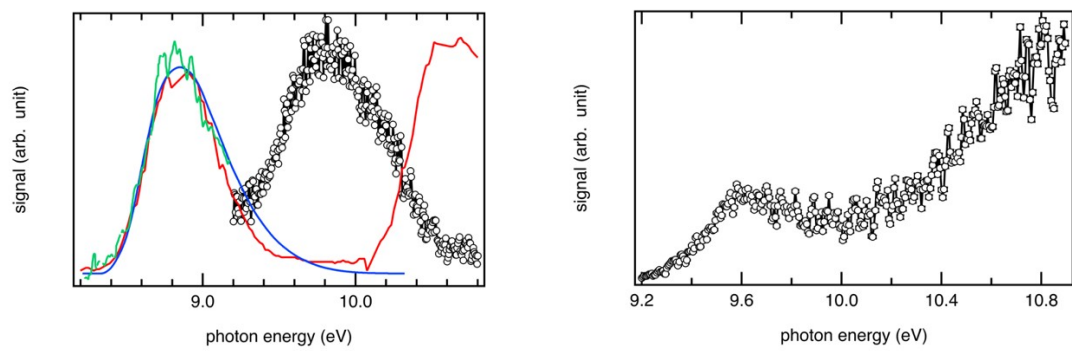


FIGURE S3. SPES of  $m/z$  146 (open circles) recorded during synchrotron photoionization of a tBuOOH/*n*-decane mixture in helium compared to a referenced PES of di-tBuO (red line) from Batich & Adam [50], a TPEPICO spectrum of di-tBuO (green line) from Shuman et al. [49], and a simulated spectrum of di-tBuO (blue line); (right) SPES of  $m/z$  73 (black dots) recorded during synchrotron photoionization of a tBuOOH/*n*-decane mixture in helium.

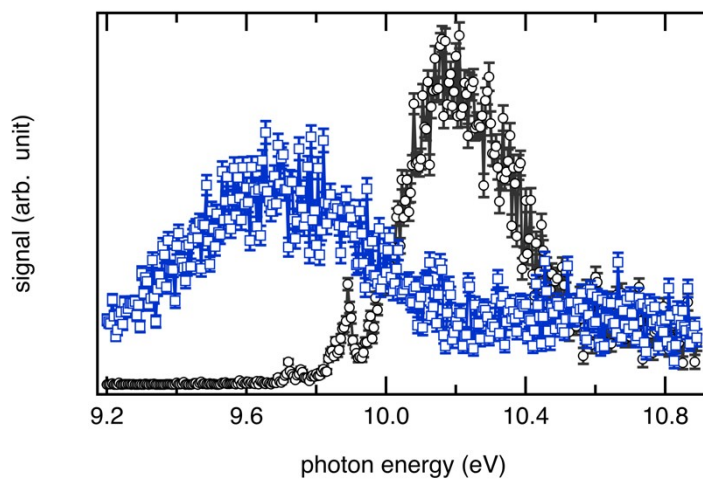


FIGURE S4. SPES of  $m/z$  59 (open circles) and 180 (blue squares) recorded during synchrotron photoionization of a tBuOOH/*n*-decane mixture in helium.

TABLE S1. PBE0/aug-cc-pVTZ optimized equilibrium geometry of neutral and cationic tBuOOH.

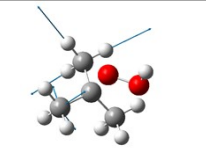
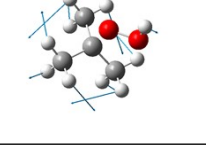
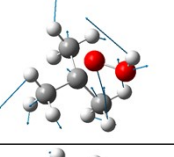
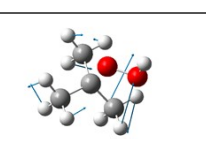
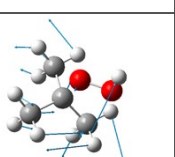
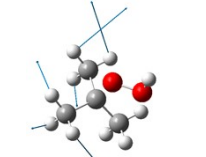
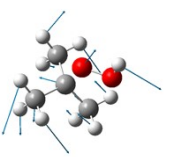
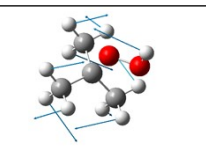
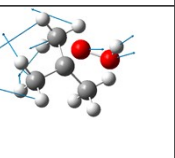
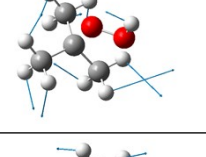
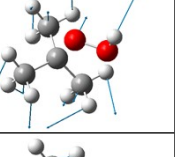
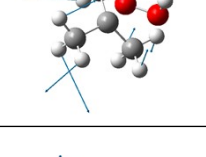
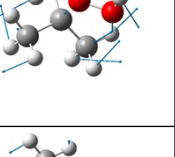
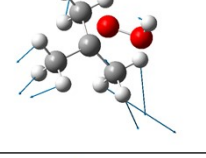
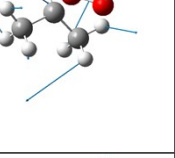
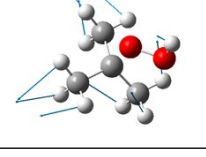
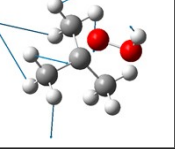
Distances are in Å and angles in degrees. See FIGURE 6 for the numbering of the atoms.

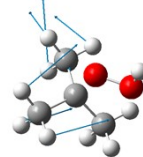
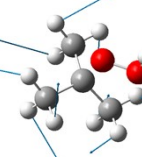
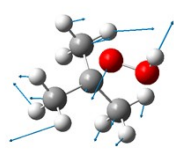
	tBuOOH	tBuOOH <sup>+</sup>
R(1,2)	1.520	1.499
R(1,6)	1.520	1.518
R(1,10)	1.520	1.518
R(1,14)	1.438	1.546
R(2,3)	1.091	1.090
R(2,4)	1.090	1.090
R(2,5)	1.092	1.091
R(6,7)	1.091	1.089
R(6,8)	1.091	1.092
R(6,9)	1.091	1.090
R(10,11)	1.091	1.092
R(10,12)	1.091	1.089
R(10,13)	1.092	1.090
R(14,15)	1.427	1.307
R(15,16)	0.963	0.982
A(2,1,6)	111.2	114.8
A(2,1,10)	111.6	114.8
A(2,1,14)	110.1	110.3
A(6,1,10)	111.1	113.0
A(6,1,14)	101.9	101.0
A(10,1,14)	110.5	100.7
A(1,2,3)	110.3	112.4
A(1,2,4)	110.7	112.4
A(1,2,5)	110.2	106.7
A(3,2,4)	108.5	109.7
A(3,2,5)	108.5	107.6
A(4,2,5)	108.4	107.6
A(1,6,7)	110.5	111.6
A(1,6,8)	109.7	106.7
A(1,6,9)	110.8	112.0
A(7,6,8)	108.5	108.5
A(7,6,9)	108.6	110.0
A(8,6,9)	108.5	107.9
A(1,10,11)	110.2	106.7
A(1,10,12)	110.9	111.6
A(1,10,13)	110.5	112.0
A(11,10,12)	107.8	108.5
A(11,10,13)	108.2	107.9
A(12,10,13)	109.0	110.0
A(1,14,15)	109.6	114.1

A(14,15,16)	101.1	103.8
D(6,1,2,3)	-55.7	-51.0
D(6,1,2,4)	-175.9	-175.5
D(6,1,2,5)	64.1	66.7
D(10,1,2,3)	179.5	175.5
D(10,1,2,4)	59.4	51.1
D(10,1,2,5)	-60.5	-66.7
D(14,1,2,3)	56.4	62.2
D(14,1,2,4)	-63.8	-62.2
D(14,1,2,5)	176.3	-180.0
D(2,1,6,7)	57.9	50.0
D(2,1,6,8)	-61.8	-68.3
D(2,1,6,9)	178.4	173.8
D(10,1,6,7)	-177.1	-175.7
D(10,1,6,8)	63.2	66.0
D(10,1,6,9)	-56.6	-51.9
D(14,1,6,7)	-59.3	-69.0
D(14,1,6,8)	-179.0	173.0
D(14,1,6,9)	61.1	55.1
D(2,1,10,11)	62.0	68.3
D(2,1,10,12)	-57.4	-50.0
D(2,1,10,13)	-178.4	-173.8
D(6,1,10,11)	-62.7	-66.0
D(6,1,10,12)	177.9	175.7
D(6,1,10,13)	56.8	51.9
D(14,1,10,11)	-175.1	-173.0
D(14,1,10,12)	65.5	68.7
D(14,1,10,13)	-55.5	-55.1
D(2,1,14,15)	60.3	0.0
D(6,1,14,15)	178.4	121.8
D(10,1,14,15)	-63.5	-122.0
D(1,14,15,16)	110.1	-180.0

TABLE S2. Anharmonic frequencies ( $\nu^+$ ,  $\text{cm}^{-1}$ ) of  $\text{tBuOOH}^+$  electronic ground state as computed at the PBE0/aug-cc-pVTZ level, using the VPT2 theory to describe the nuclear motions as implemented in GAUSSIAN 16. We also give their tentative assignment in terms of normal modes and atomic displacements. v: stretching;  $\delta$ : bending;  $\gamma$ : rocking;  $\tau$ : torsion. s: symmetric; and as: asymmetric.

mode	$\nu^+$	Assign.	Displ.	mode	$\nu^+$	Assign.	Displ.
1	3413.0	v(OH)		22	1196.5	v(CC)	
2	3026.4	v(CH <sub>3</sub> ) s		23	1189.9	v(OO)	
3	3026.1	v(CH <sub>3</sub> ) as		24	1085.1	$\gamma(\text{CH}_3)$	
4	3022.3	v(CH <sub>3</sub> ) as		25	1023.1	$\gamma(\text{CH}_3)$	
5	3022.4	v(CH <sub>3</sub> ) s		26	993.4	$\gamma(\text{CH}_3)$	
6	3011.9	v(CH <sub>3</sub> ) s		27	963.2	$\gamma(\text{CH}_3)$	
7	3018.0	v(CH <sub>3</sub> ) as		28	907.7	$\gamma(\text{CH}_3)$	
8	2956.9	v(CH <sub>3</sub> ) s		29	903.3	$\gamma(\text{CH}_3)$	
9	2946.8	v(CH <sub>3</sub> ) s		30	754.3	v(CC)	

10	2939.6	$\nu(\text{CH}_3)$ s		31	573.1	$\delta(\text{OOH})$	
11	1464.6	$\gamma(\text{CH}_3)$		32	524.0	$\gamma(\text{OOH})$	
12	1446.9	$\delta(\text{OOH})$		33	407.5	$\nu(\text{CO})$	
13	1440.4	$\gamma(\text{CH}_3)$		34	394.9	$\gamma(\text{CH}_3)$	
14	1428.7	$\gamma(\text{CH}_3)$		35	342.6	$\nu(\text{CO})$	
15	1421.4	$\gamma(\text{CH}_3)$		36	299.1	$\delta(\text{CCC})$	
16	1409.2	$\gamma(\text{CH}_3)$		37	310.6	$\delta(\text{CCC})$	
17	1405.2	$\gamma(\text{CH}_3)$		38	272.6	$\delta(\text{OOC})$	
18	1391.3	$\nu(\text{CC})$		39	273.2	$\tau(\text{C-C})$	
19	1360.7	$\gamma(\text{CH}_3)$		40	232.2	$\tau(\text{C-C})$	

20	1353.2	$\gamma(\text{CH}_3)$		41	178.3	$\tau(\text{C-C})$	
21	1251.8	$\nu(\text{CC})$		42	23.7	$\delta(\text{OOH})$	

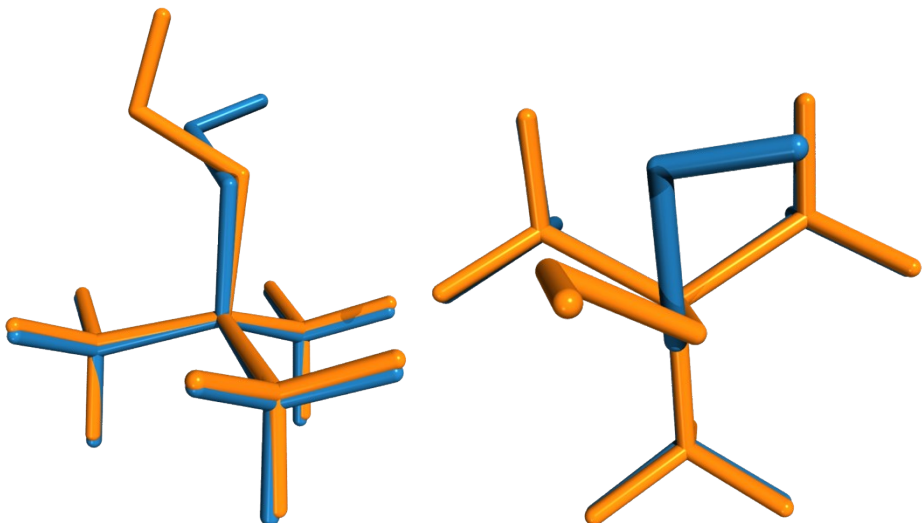


FIGURE S5: Overlapping optimized structures of tBuOOH (blue) and tBuOOH<sup>+</sup> (orange) at the PBE0/aug-cc-pVTZ levels. The 4 carbon atoms were used in the mass-weighted superposition procedure.

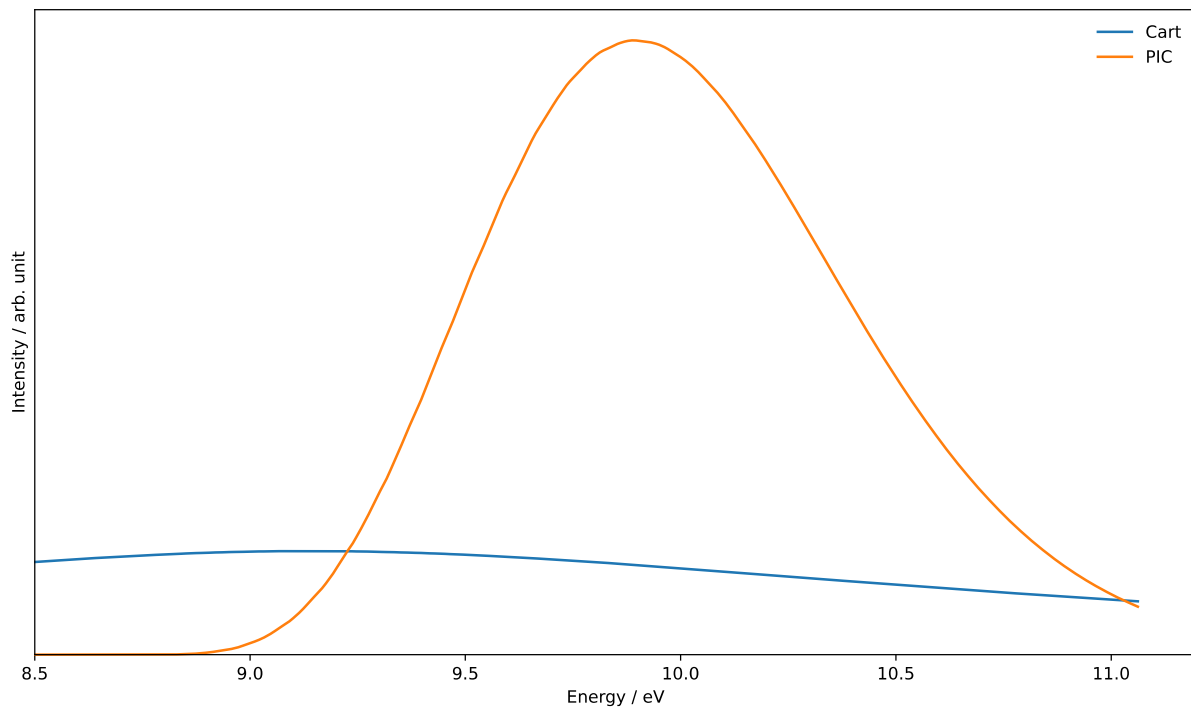
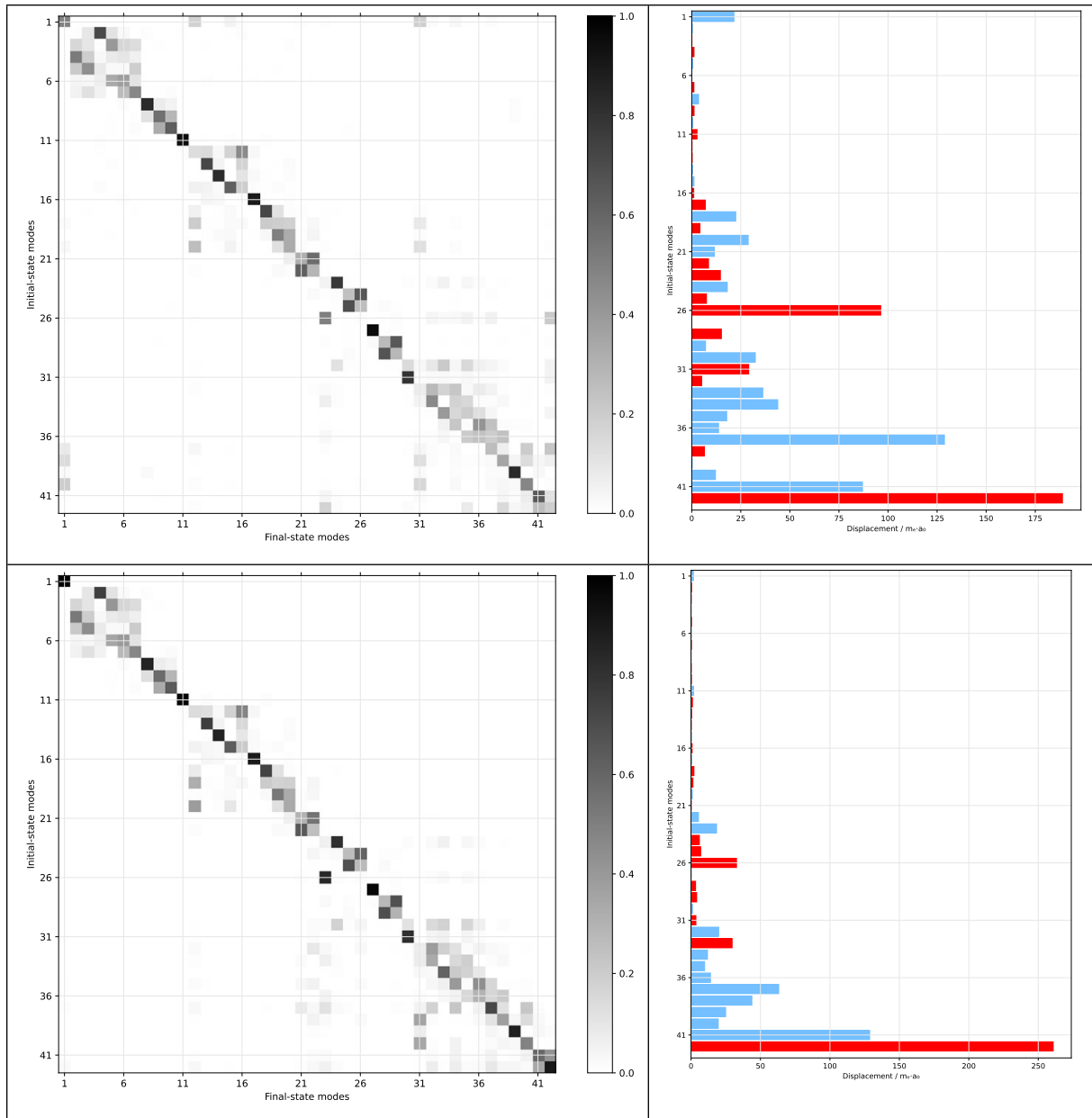


FIGURE S6: Full-dimensional PES spectrum at the FC level using the time-dependent formalism at 0K using Cartesian-based (Cart) or internal-based (PIC) normal coordinates. Gaussian distribution functions with HWHMs of 20 meV were used for the empirical broadening.



**FIGURE S7:** Duschinsky matrix (left panels) and shift vector (right panels) relative to the PES spectrum of tBuOOH at the PBE0/aug-cc-pVTZ level. In the top panels, Cartesian coordinates are used for the definition of the normal modes. In the bottom panels, the basis are primitive internal coordinates. The Duschinsky matrix ( $J$ ) is represented by squaring each element and attributing a shade of gray based on its value (0: white, 1: black). For the shift vector ( $K$ ), the absolute value is displayed to compare the magnitude of the shift along each normal coordinate. A blue color indicates a positive value, red for negative.

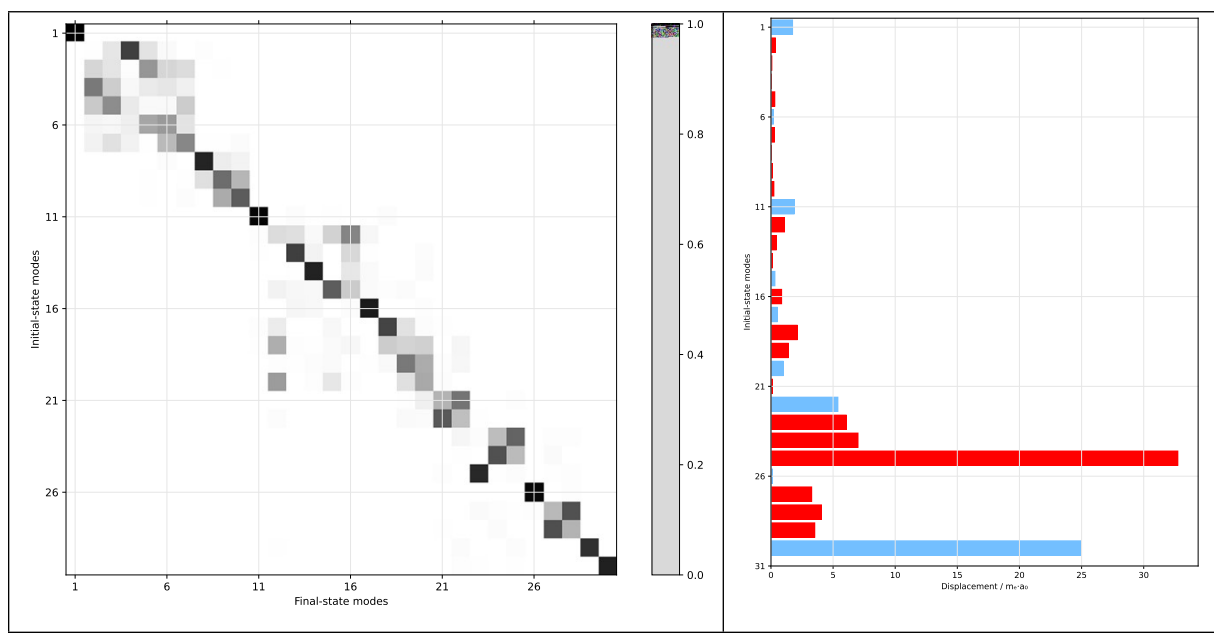


FIGURE S8: Duschinsky matrix (left panels) and shift vector (right panels) relative to the PES spectrum of tBuOOH at the PBE0/aug-cc-pVTZ level for the final reduced-dimensionality scheme. See FIGURE S7 for details.